Fall Technical Meeting of the Eastern States Section of the Combustion Institute
Hosted by the University of Connecticut, Storrs, CT
Oct 9-12, 2011

On Self-Acceleration of Cellular Spherical Flames

Fujia Wu, Grunde Jomaas and Chung K. Law

Department of Mechanical and Aerospace Engineering, Princeton University, Princeton, New Jersey 08544, USA

An expanding spherical flame is hydrodynamically unstable in the flame-sheet limit, attained either as the flame reaches a sufficiently large dimension as compared to the flame thickness, and/or when it propagates in a high-pressure environment such that its thickness is correspondingly reduced. The cells that continuously develop over the flame surface increase its area and thereby the global propagation rate, resulting in the possibility of self-acceleration. The present study examines whether this self-acceleration could be self-similar, and if so whether it could also be self-turbulizing. A critical appraisal of the experimental and computational results in the literature on these issues was performed, and experiments were conducted for hydrogen/air mixtures over an extensive range of elevated pressures. Results demonstrate the strong possibility of self-similar flame acceleration, moderate influences of diffusional-thermal instability and of the system pressure, and a corresponding moderate spread in the power-law acceleration exponent.

1. Introduction

Propagation of laminar premixed flames is subjected to the excitation of flamefront hydrodynamic, diffusional-thermal, and buoyancy instabilities, which are respectively caused by the density jump across the flame, the non-equidiffusive nature of the diffusive scalars of species concentration and heat, and body force in the presence of density gradient. The presence of cells over the flame surface increases its surface area and consequently also the global propagation speed of the flame. Furthermore, since new cells continuously evolve, it is reasonable to expect that the flame speed will also continuously increase, leading to the possibility of self-acceleration. The phenomenon is of particular interest for the propagation of the globally spherical flame because of the essentially well-defined, yet continuously increasing flame radius, which yields a characteristic dimension and the dynamic parameters against which excitation of the various instability modes evolve. Specifically, during the initial stage of flame propagation when the flame radius is small, the small-scale diffusional-thermal instability is expected to dominate. As the flame becomes larger and the flame thickness is small compared to the flame radius, the hydrodynamic, Darrieus-Landau instability sets in, progressively dominating the flame morphology and the accelerative dynamics. Finally, the accelerative motion and the continuously increasing flame dimension will eventually activate the radially directed, large-scale, Rayleigh-Taylor, body-force instability.

This self acceleration can be quantified, and an assessment of the propagation mode made, by determining the history of the average flame radius, R_{av}, through a power-law expression,

$$R_{av} \sim t^{\alpha}$$

There has been considerable interest in the specific values that α can assume. That is, if α is a constant, then the flame acceleration is either self-similar in t, if it holds for all t, or locally similar if it holds only for a specific period of t. Furthermore, it has been suggested [1-3] that if α is not an integer, then the wrinkled flamefront can be considered as a fractal surface with the total surface area of the front given by,

$$A_f \sim R_{av}^{2+d}$$

where the constant $d = 1 - 1/\alpha$ is the factual excess. In the limit of an infinitesimally thin flame, diffusional-thermal effects are suppressed and the local flame speed over the wrinkled flame surface is that of the laminar flame speed, S_L, and as such is a constant. The fractal hypothesis then leads to the self-similar propagation of the flamefront,

$$4\pi R_{av}^{\ 2} \frac{dR_{av}}{dt} \approx S_L A_f$$

$$\frac{dR_{av}}{dt} \sim R_{av}^{\ d}$$

Finally, for fully-developed Kolmogorov turbulence it has been suggested by Mandelbrot [4,5] that the iso-surfaces (such iso-temperature) also have fractal character, and the fractal excess d has been theoretically estimated by Sreenivasan *et al.* [6] based on Reynolds number similarity to be $1/3$. Experimental values by Sreenivasan *et al.* [7,8] for a variety of turbulent flows fall in the range of 0.35 ± 0.05, a close agreement to $1/3$. For the case of expanding laminar flame under hydrodynamic instabilities, if α also assumes the value of $3/2$, then $d = 1/3$, and the flame has possibly undergone self-turbulization and thereby having the character of turbulence.

Considerable experimental and theoretical studies have been conducted aiming to demonstrate the possible attainment of $\alpha = 3/2$ and hence self-turbulization, although with inconclusive results. In fact, in the interest of demonstrating such an attainment, interpretations of the theoretical and experimental results have been conducted rather loosely, causing considerable confusion in the rigorous understanding of the phenomena.

In view of the above considerations, the present study has two objectives. First, we shall conduct a fairly rigorous overview of the literature on the state of the determination of α, demonstrating that the various claims of $\alpha = 3/2$ are far from justified. Second, we shall perform a well-controlled experimental investigation, aiming to provide reliable data to answer the following three increasingly demanding claims on α, namely:

- Does the flame self-accelerate, *i.e.*, $\alpha > 1$?
- Is α a constant such that the propagation is self-similar?
- Is α approximately equal to $3/2$ such that the wrinkled flame self-turbulizes?

2. Review of Previous Works

2.1 Experimental Studies

Lind and Whitson [9] conducted large-scale explosion experiments in quiescent condition at atmospheric pressure with various mixtures including H_2/air, H_2/O_2, C_3H_8/air, CH_4/air, C_4H_6/air, C_2H_2/air. These experimental data were later analyzed by Gostintsev *et al.* [10], who concluded that α is a constant and its value is $3/2$ for all mixtures under studied. The data analysis was

however not clearly described and the time resolution of the data was also poor. Only a few data points were plotted for each curve, as shown in Figure 1. It is also noted that the right plot in Figure 1, for H_2/air and H_2/O_2, shows that the slope of $R-t^{3/2}$ of most curves jumps in the middle, indicating two different regimes of self-similar propagation, with two distinct values of α. In addition, in two follow-on publications [11,12] the original reported value of $\alpha=1.5$ was lowered to 1.25~1.5, with the revised assessment that the value of 1.5 is only attained in limiting cases.

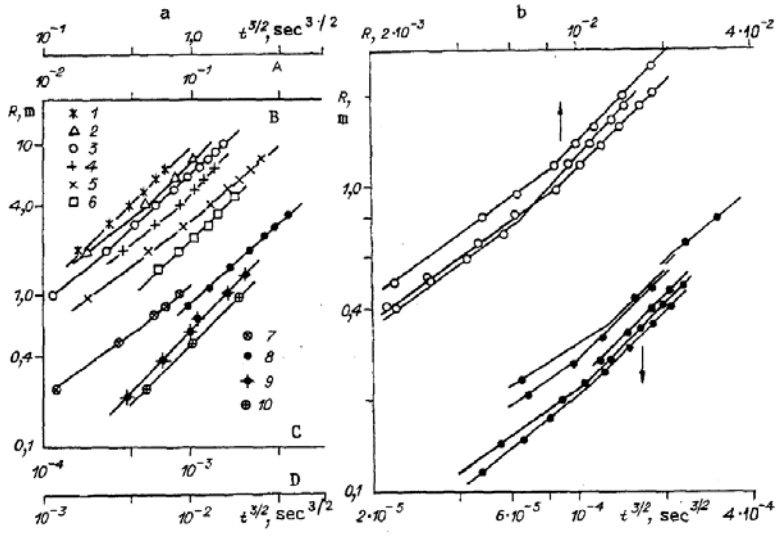

Figure 1: Flame radius, *R*, versus time, t, to the power of 3/2 in Ref. [10]

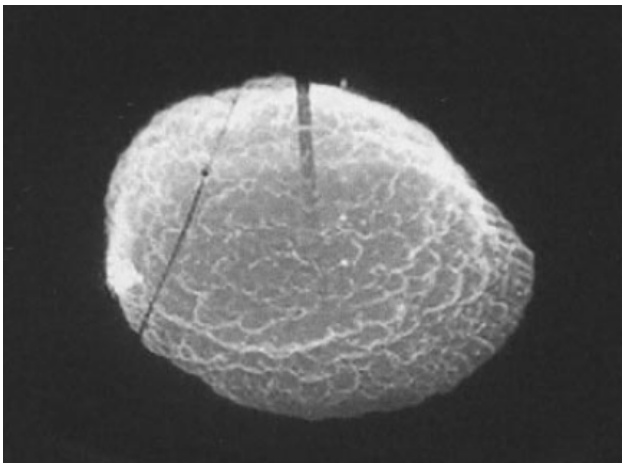

Figure 2: Flame photograph in Ref. [13], largely distorted from spherical shape by buoyancy

Bradley *et al.* [13] experimented with large-scale flames, allowing outwardly the propagating flame to grow to radius as large as 3 meters at atmospheric pressure so that hydrodynamic cells could be developed under such condition. Based on their data, a constant α of 1.5 was again reported. However, due to strong buoyancy with typical Froude numbers, V^2/gR, being around 2, the experimental flame was basically hemispherical, as shown in Figure 2. The severe lack of

spherical symmetry fundamentally complicates the data interpretation and analysis, and consequently the rigor of the quantitative value reported.

Haq [14] conducted experiments for CH_4/air atmospheric flames in a combustion vessel. It was shown that the data obtained at small radii could be blended with those of Lind and Whitson [9] at large radii, with good match (Figure 3). Furthermore, the results showed that α is 1.24 for the horizontal radii and 1.32 for the vertical radii; this difference could be due to buoyancy effects. The primary concern with this series of experiments is whether mature hydrodynamic cells were developed for flames of such small dimensions at atmospheric pressure, at which the flame thickness would require cells of large dimensions, recognizing that the flame of Bradley *et al.* [13] required 3 meters to develop.

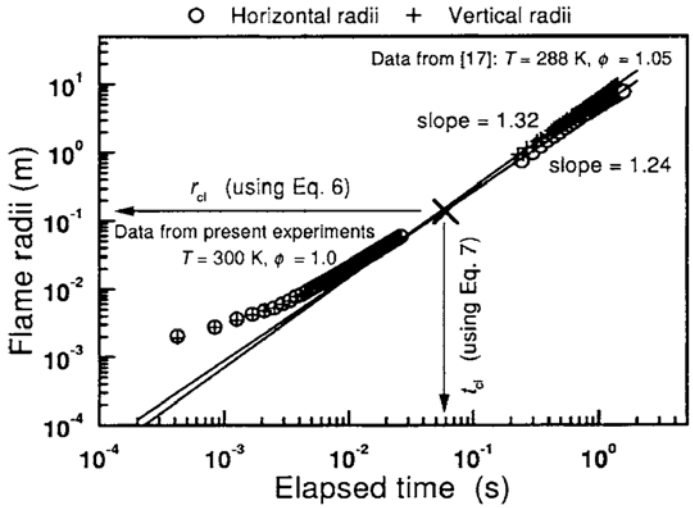

Figure 3: Flame radius versus time for experiment in Ref. [14] and Ref. [9].

Kwon *et al.* [15] experimented with $H_2/O_2/N_2$ flames, using a constant and high pressure dual-chamber vessel at a pressure of 15 atm. It is noted that the elevated pressure reduces the flame thickness and thereby the hydrodynamic cell size, hence allowing the development of hydrodynamic cells for the small, laboratory-scale flames. The reported values of α is 1.26, 1.36 and 1.23 for ϕ = 0.5, 1.0 and 1.5 respectively.

2.2 Numerical Studies

A number of numerical investigations have been conducted, with focus on the issue of self-acceleration of expanding wrinkled flames. Due to the computational cost, almost all studies were performed for the 2-D cylindrical flames. Since the power-law exponent α for the 2D and 3D flames are necessarily different, as noted by Blinnikov and Sasorov [2], caution is needed in drawing direct comparison for values of α obtained from 2D and 3D flames. Furthermore, most simulations were also conducted using simplified models, such as the Sivashinsky equation or Frankel equation. Finally, several studies claimed the existence of $\alpha_{2D} = 1.5$ by drawing straight lines over results with large curvatures.

With the above cautionary comments, we note that Filyand *et al.* [16] considered a modified version of the Sivashinsky equation on a 2-D outward propagating flames, and reported $\alpha_{2D} = 1.5$. Subsequently Ashurst [17] performed 2-D Lagrangian simulations with a potential

flow model, and also reported a power-law with $\alpha_{2D} = 1.5$. Similarly, Aldredge and Zuo [18] used a level-set formulation and Euler equation to simulate 2-D expanding flames, and again reported a constant of $\alpha_{2D} = 1.5$.

Blinnikov and Sasorov [2] simulated 2-D expanding flames with the Frankel equation by considering the limiting case of small thermal expansion, *i.e.*,

$$\gamma = \frac{\rho_u - \rho_b}{\rho_u} << 1$$

and found that the fractal excess $d_{2D} = 1 - 1/\alpha_{2D}$ depends on γ through the following relationship

$$d_{2D} = 0.3\gamma^2$$

Assuming that this result holds for the realistic values of γ between 0.8~0.9, then we have d_{2D} = 0.19 ~ 1.24 and α_{2D} = 1.24 ~ 1.32.

Olami and co-workers [19-21] numerically simulated 2-D expanding flames with a modified Sivashinsky equation, and suggested that α_{2D} = 1.65$\pm$0.1 in the initial period of propagation, and developed to a saturated value of 1.35$\pm$0.03, as shown in Figure 4. It was also commented that the effect of artificial numerical noise is crucial in the study of accelerating and wrinkled flamefronts.

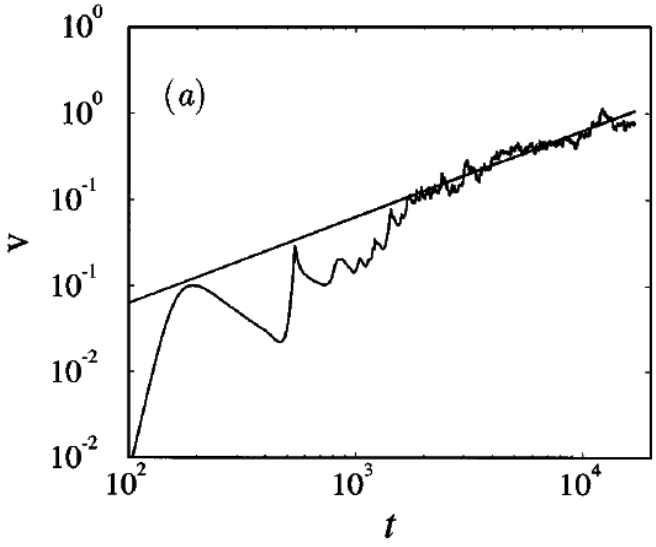

Figure 4: Flame propagation velocity versus time for the simulation in Ref. [21]

Liberman *et al.* [22] performed 2-D simulations by means of directly solving the N-S equations with 1-step Arrhenius chemistry. Their results showed a power-law behavior with α_{2D} = 1.25 after the flame travels through an initial period of high values of α_{2D} (Figure 5). They also commented that 2-D and 3-D results should be different.

Karlin and Sivashinsky [23,24] simulated both 2-D cylindrical and 3-D spherical expanding flames using the Sivashinsky equation. The 2-D simulation results confirmed the fractal theory of accelerating expanding flames: α_{2D} reaches a saturated value of 1.25$\pm$0.03 after an initial

period. The 3-D simulation used a simplified asymptotic model which greatly reduced the computation time. The simulation was able to output realistic looking flamefront as shown in Figure 6; the results, however, showed a non-constant α_{3D} (see the curve indicated by star and circle solid lines in Figure 7), with α_{3D} between 1.76 and 1.9. The author nevertheless indicated that after some transitional period the acceleration still has a good chance to reach the 1.5-power-law.

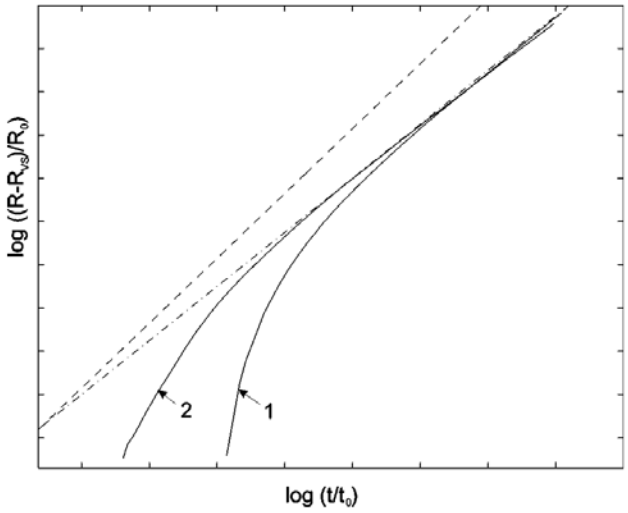

Figure 5: Normalized flame radius versus time for two sets of simulations in Ref. [22]

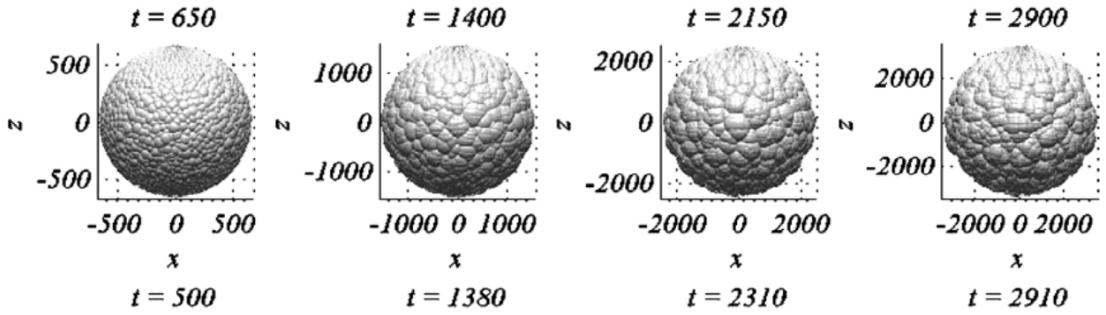

Figure 6: Flame shape in the 3-D simulation in Ref. [24]

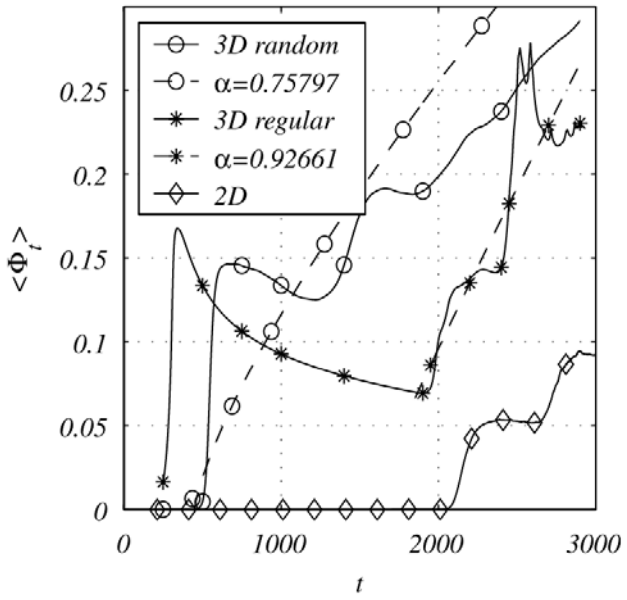

Figure 7: Flamefront propagation velocity versus time in the simulation in Ref. [24]

Pan and co-workers [25,26] simulated 2-D flames using the Sivashinsky equation with a random forcing term. The results showed that the acceleration exponent depends on the thermal expansion ratio. For realistic thermal expansions, the value of α_{2D} is between 1.25 and 1.5. It was also commented that there is uncertainty in evaluating α_{2D} through different fitting methods on the $R-t$ curve.

2.3 Fitting Formulas

In addition to disagreement in the values of α, there is also inconsistency among different studies in the extraction of α. The early studies of Gostintsev [10] and Bradley [13] simply assumed $\alpha = 1.5$ and applied the following self-similar law:

$$R = R_0 + At^{3/2}$$

where R is the flame radius and t the time after ignition, R_0 and A are the parameters for best linear fitting. Such a fitting of course automatically assigns $\alpha = 1.5$, although an examination of their data shows that a plot of $R-t^{3/2}$ is not exactly linear, and that the time resolution of the data was too poor to make conclusions.

To evaluate α directly from data, other experimental and numerical studies [15,17,22] treated all R_0, A and α as fitting parameters:

$$R = R_0 + At^{\alpha}$$

where R is flame radius and t is the time after ignition in experiments or the time after calculation starts in the simulation. This formula allows one to quantify the acceleration exponent α directly from data. However, because of the definition of t, the fitting result will automatically depend on the instant of ignition or the simulation starting point. For example, as shown in Figure 8, when a set of experimental data is artificially shifted in time (which can be caused by the different ignition conditions among different experiments), different values of α are obtained.

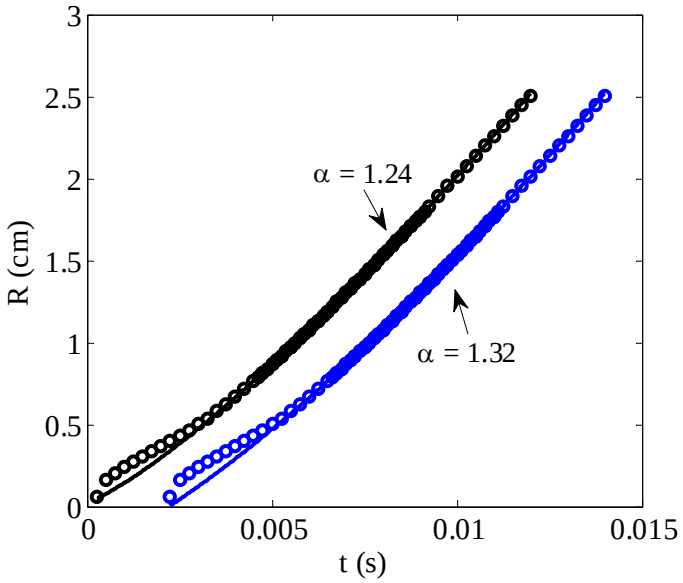

Figure 8: A set of experimental data in the present study; Black: original data, Blue: same set of data after an artificial time shift. Filled circles indicate data used for fitting.

Some other studies [16,18] set R_0 to be the visual onset of the transition from a smooth to a wrinkled flame, and consider the following formula:

$$R = R_0 + A(t - t_0)^{\alpha}$$

where R_0 and t_0 are the radius and time of the onset of wrinkling. This method avoids the influence of the ignition condition; however, it introduces two other concerns. First, the determination of the onset of celluarity from experiment or numerical flame images is quite subjective. The fitting result depends on values of R_0 and t_0 sensitively, especially for the range of data point that immediately follow the onset since both $R - R_0$ and $t - t_0$ are close to zero. Second, since there is possibly a transitional period after the onset for the acceleration to reach a saturated self-similar regime, shown in the present data as well as some numerical simulations [21-23], using this formula still depends on the transitional period.

Some numerical studies [21,23,24] fitted the calculated propagation velocity $U = dR/dt$ by a power-law

$$U = A\alpha^{-1}t^{\alpha-1}$$

while others [14] ignored the constant R_0 or t_0 and directly considered the power-law

$$R = At^{\alpha}$$

However, the influence of initial condition still exists as t is still defined as the time after ignition in experiments or time after calculation starts in simulation.

3. Present Experiment and Data Analysis

3.1 Experimental Considerations and Specifications

Extensive experiments have been previously conducted at high initial pressures in closed vessels, primarily for the determination of laminar flame speeds of combustible mixtures. These vessels are typically windowless because optical windows may not withstand the excessively high post-combustion temperature and pressure. The lack of observation then severely compromises their utility for the study of flamefront instabilities. Recently windowed vessels have been constructed and studies have been conducted at moderately high initial pressures, say up to 10 atmospheres. Useful data from such studies are however limited to the early period of flame propagation, when the flame size is small compared to that of the vessel. This limitation arises because the vessel pressure and the unburned mixture temperature continuously increase as the flame propagates, with the increase being quite substantial when the size of the growing flame ceases to be small compared to that of the vessel. This therefore renders flame propagation to be essentially transient, whose effect cannot be readily filtered out. This complication is particularly restrictive for the present study because we are interested to identify the transient effect caused by the growth of the cells over the flame surface.

The above restrictions have recently been removed in a new, dual-chamber design of the combustion vessel that allows observation of constant-pressure flame propagation with initial pressures as high as 60 atmospheres. Using this apparatus, useful observations have been made on the characteristics of the propagation of cellular flames, including the transition threshold of hydrodynamic and diffusional-thermal instabilities in expanding spherical flames.

Procedurally, the reactant mixture was prepared in an inner chamber through partial pressures; while the outer chamber was filled with inert gases whose density matches that of the gas in the inner chamber. Two sleeves with holes that were offset relative to one another initially separated the two chambers. Immediately prior to ignition, one sleeve was impulsively slid over the other so that the holes became aligned, allowing the gas in the inner chamber to pass through as the flame propagates. The mixture was spark-ignited at the center of the inner chamber, and was subsequently quenched as it reached the separating sleeve, thus preventing the attainment of the large pressure rise usually associated with conventional single chamber designs. Since the volume of the outer chamber is 25 times that of the inner chamber in the present design, the pressure rise has been measured to be less than 3% for the entire chamber. Furthermore, for the small radii in the current study, the actual pressure rise is significantly smaller, providing an almost constant pressure combustion process. The flame propagation was imaged with schlieren photography and recorded using a high-speed digital camera at 8,000, 15,000, or 25,000 frames per second, depending on the propagation speed of the flame.

Hydrogen was used as the fuel because of its thin flame thickness. In earlier studies, we have determined the instant of the onset of instabilities for a wide range of expanding flames, and compared the results with theory. It was demonstrated that all flames at elevated pressures eventually become unstable, in accordance with Landau's theory of hydrodynamic instability formulated in the limit flame-sheet combustion. Furthermore, flames with $Le<1$ reach the cellular mode of propagation at smaller radii, while the opposite holds for the $Le>1$ flames. Recognizing that hydrogen flames propagate faster and are thus thinner than hydrocarbon flames, and that the Lewis numbers of their lean mixtures are also much smaller than unity, lean hydrogen flames were observed to almost immediately exhibit cellular instabilities after initiation of propagation. Consequently they are particularly suitable for the present investigation, with their cellular propagation mode taking place over 10^2 to 10^3 flame thicknesses

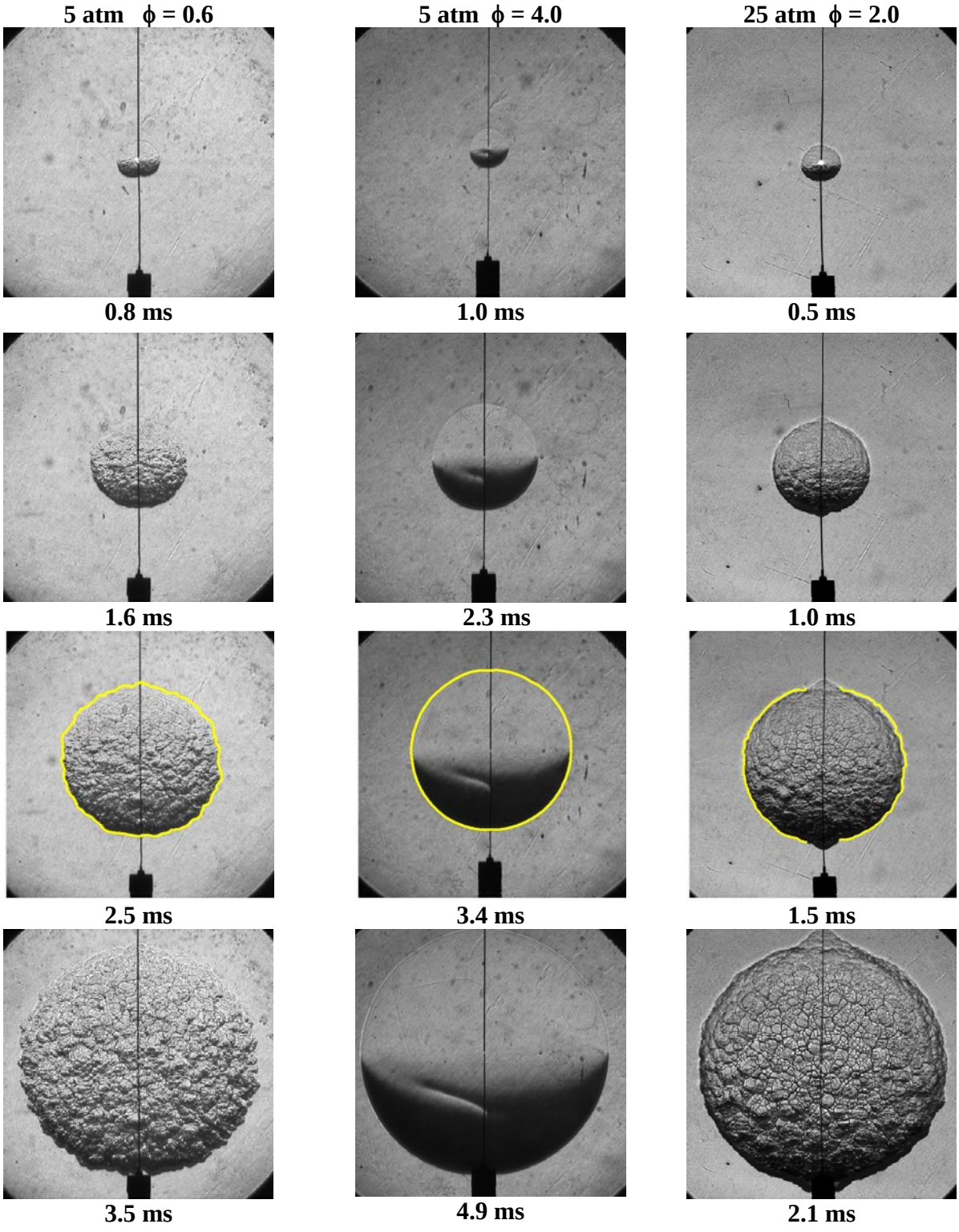

Figure 9: Sequences of flame propagation in hydrogen/air mixtures, showing the development of cellular flamefront instability is promoted for *Le* < 1 mixtures (ϕ = 0.60, P = 5 atm) and in high pressure environments (ϕ = 2.0, P = 25 atm)

in our investigation. This provides ample time and space for the development of the cell size and exploration of the possible existence of a self-similar propagation mode.

3.2 Data Processing

Figure 9 shows three typical sequences of the images of propagating hydrogen/air flames. Specifically, it is seen that, at 5 atm pressure, the flame surface is wrinkled for lean but not rich mixtures, hence demonstrating the destabilizing effect of the diffusional-thermal instability on the lean mixture whose Le is less than unity. Flames of the rich mixtures, however, also become wrinkled at the higher pressure of 25 atm, demonstrating the manifestation of the hydrodynamic instability as the flame becomes thinner with increasing pressure.

Accurate tracking of the flamefront from Schlieren cine images has been shown to be crucial, especially for a subject like this current study with high sensitivity. Since wrinkled flamefronts contain many troughs and cusps, only averaged flame radius of the entire flamefront has statistical meaning. In this study, the Canny Edge Detection method was applied on the experimental flame images and the flame radius $R(\theta,t)$ was determined as a function of time, t, and angle, θ. The tracked lines are plotted in the third row of each column in Figure 9. The flame evolution contour of $R(\theta,t)$ is also plotted in Figure 10. It is noted that due to limitation of the spatial resolution of these images, the contour of $R(\theta,t)$ does not contain the cell formation on small scales, therefore a fractal analysis based on the flamefront geometry as in [16] was not conducted in this study.

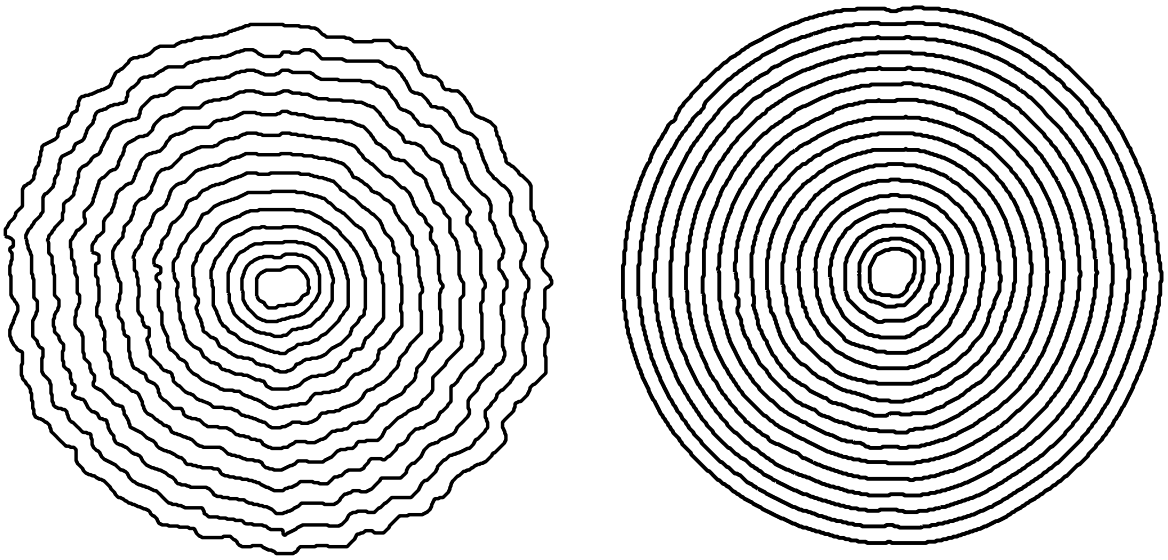

Figure 10: Contour of tracking result of a wrinkled flame at ϕ = 0.4, P = 5 atm (left) and a smooth flame at ϕ = 4.0, P = 5 atm (right)

From the tracking results, the average flame radius of a wrinkled flamefront is defined as,

$$R_{av}(t) = \int_0^{2\pi} R(\theta, t) d\theta$$

It is noted that sometimes the ignition wires deform the flamefront locally, for example, the third column of Figure 9. For these flames, the section of flamefront with an odd shape around the ignition wires was deleted in the tracking, as shown in yellow line in the images at the third row.

Realizing that inconsistency in the fitting method among previous studies on this manner, we note that the fundamental hypothesis on the self-similar propagation is applied to the velocity instead of the radius [1,2],

$$U_{av} = \frac{dR_{av}}{dt} = BR_{av}^{d}$$

where $B = \alpha A^{1/\alpha}$ is a constant that only depends on the properties of the mixture. This relation directly comes from the fractal description of the flame propagation. Therefore this formula is employed in this study, treating B and d as parameters for best fitting. The current fitting method therefore removes the influence of initial condition through removal of t in the fitting equation, and the issues in the determination of R_0 or t_0.

The only concern remaining is then the accuracy in the numerical differentiation of R_{av} to obtain U_{av}. For any discrete data, direct numerical differentiation, for example center differencing, will introduce additional random error. For example, in a number of previous studies [14,16,21,26], although the $R-t$ plot is smooth, the $U-t$ plot is often quite scattered after the differentiation. This is either because the time step in the differentiation is too small to acquire statistically meaningful quantity, or the poor performance of the flamefront tracking technique. It is often difficult to understand the flame propagation history from the scattered velocity plots, especially considering that there is likely a transient period after cellularity onset before the acceleration reaches the self-similar regime. To suppress the random error introduced by numerical differentiation, smoothing techniques are frequently employed. However, these techniques, such as the spline fit or moving average uses a much longer range of $R-t$ data than central differencing and thus potentially can produce artificial effects, especially considering that the influences of ignition and wall confinement are to be eliminated. With these considerations, in this study we do not use any curve smooth technique: U_{av} is calculated by taking center difference on $R_{av}-t$. Owing to the quality of flamefront tracking and the fact that the entire flamefront (except the part influence by the ignition wires) is used in calculating R_{av}, the spatially local effects caused by each cusp or trough approximately cancel out. For the time step between each camera exposure in the experiment (typically 0.06~0.13 ms), a good statistically meaningful propagation velocity is automatically captured. Therefore the resulting velocity curve is reasonably smooth. If the radius is measured locally, say in the horizontal direction, the resulting velocity curve is much more scattered as shown in the comparison in Figure 11.

4. Results

In this study we are first interested to assess if the propagation of wrinkled flames really self-accelerates and if the acceleration follows a self-similar law. In other words, if we fit the velocity data with a power-law formula, the exponent α not only should be greater than unity but it should also be a constant, at least within a certain stage of the propagation. This question is

important in its own right, and needs to be addressed before the specific values of α are considered.

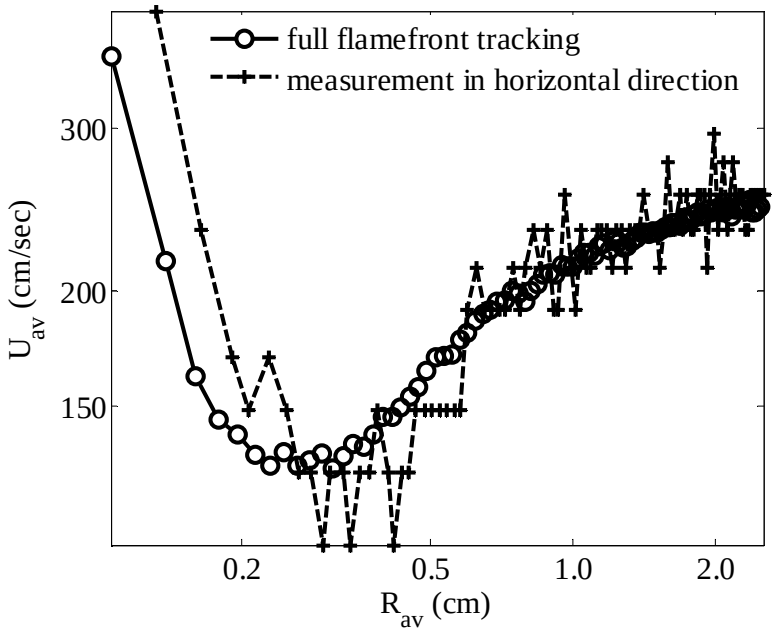

Figure 11: Comparison of velocity curves calculated from full flamefront tracking and that measured in one direction (condition: ϕ=0.4, P = 7 atm)

4.1 Self-similar Propagation Regime

Figure 12 plots the propagation velocity versus flame radius in the logarithmic scale for two experiments with the same mixtures but different ignition energies. It is seen that the two curves overlap after certain transition periods. In the overlapping region, the slope of the $\log(U_{av}) - \log(R_{av})$ remains a constant until chamber confinement starts to have an influence. This result therefore suggests that a self-similar regime does exist for wrinkled flame propagation, after a transition period. Note that in the transition period the slope is higher than that in the self-similar regime, which agrees with the numerical studies of Refs. [21,23]. The similar phenomenon was also observed for other conditions; some representative results are shown in Figures 13-15.

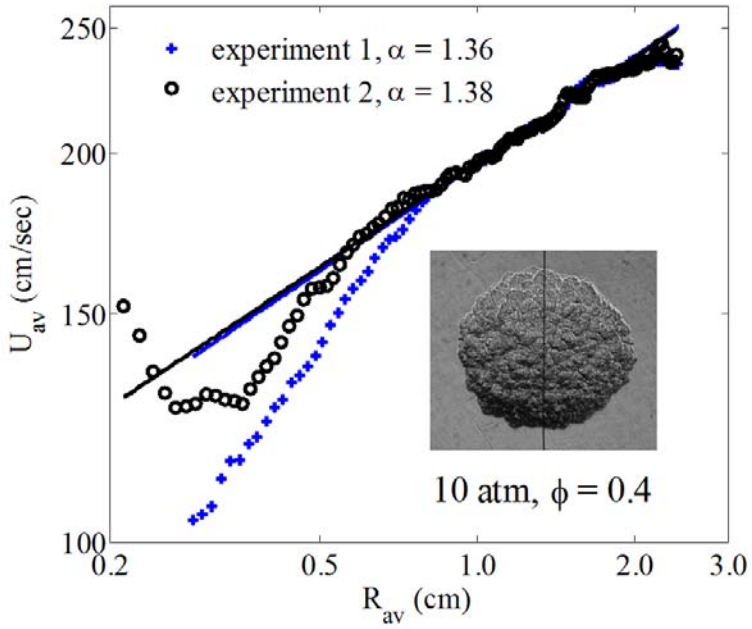

Figure 12: Propagation velocity for two experiments for H_2/air, at 10 atm, ϕ = 0.4 with different ignition conditions

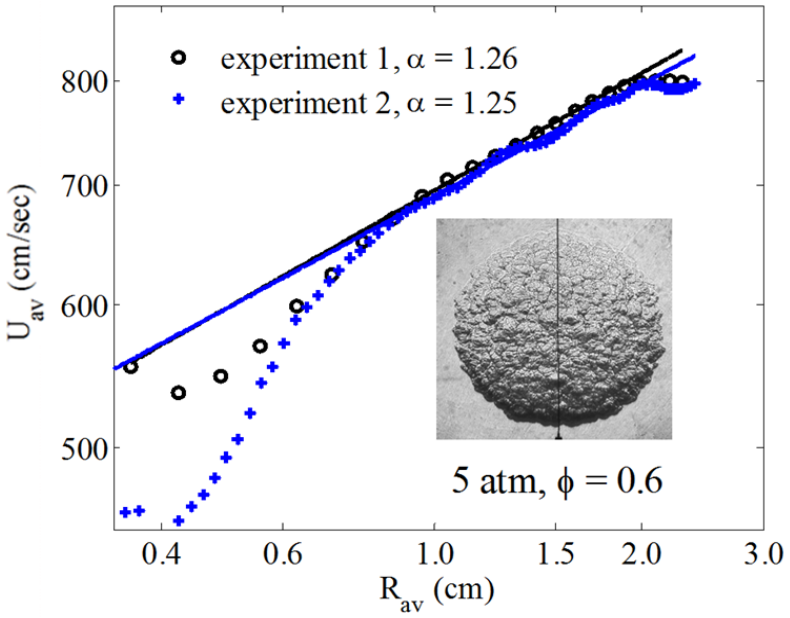

Figure 13: Propagation velocity for two experiments for H_2/air, at 5 atm, ϕ = 0.6 with different ignition conditions

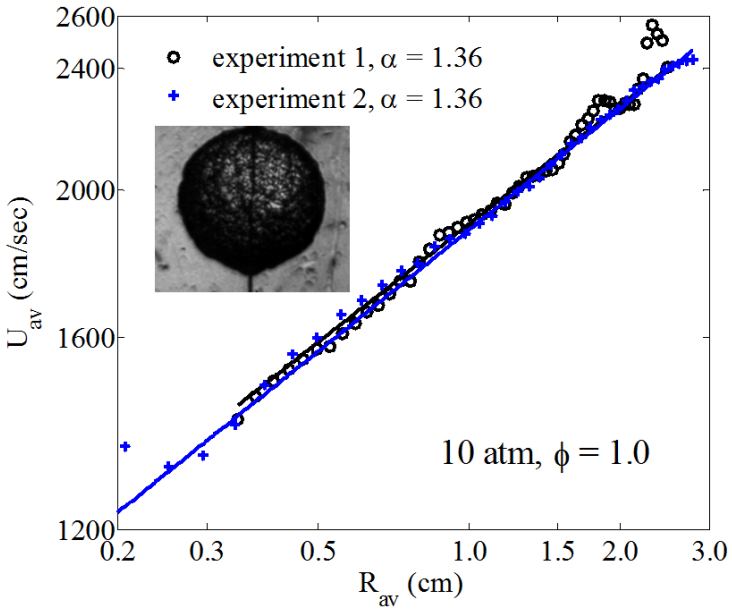

Figure 14: Propagation velocity for two experiments for H_2/air, at 10 atm, ϕ = 1.0 with different ignition conditions

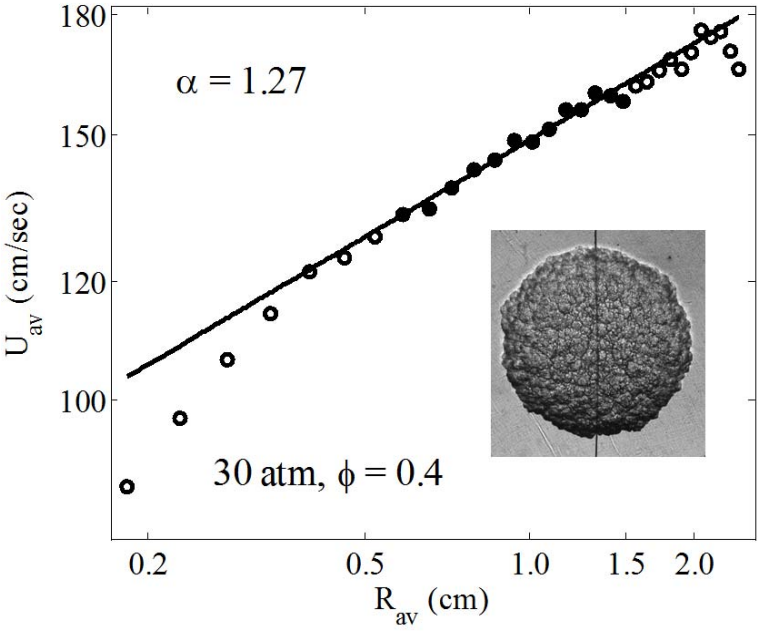

Figure 15: Propagation velocity for two experiments for H_2/air, at 30 atm, ϕ = 0.4 with different ignition conditions

4.2 Acceleration Exponents and Fractal Dimensions

In Figure 16 we plot the experimentally measured acceleration exponent α for hydrogen/air mixtures as a function of the fuel equivalence ratio, ϕ, for various pressures. Two trends are observed. First, the values of α for the lean mixtures as a group are higher than those for the rich mixtures. It is reasonable to suggest that this is due to the effect of diffusional-thermal instability, which is de-stabilizing for lean mixtures and stabilizing for rich mixtures, and as such leads to stronger and weaker wrinkling for these mixtures respectively. The second trend is that, for the strongly burning mixtures, with ϕ ranging from 0.6 to 1.2, increasing pressure results in larger values of α, which implies more wrinkling. This is in agreement with our anticipation in that, for a given ϕ, increasing pressure reduces the flame thickness and thereby increases the propensity of the flame to become hydrodynamically unstable, leading to earlier onset, and possibly more wrinkling.

This promoting effect of pressure, however, becomes less conclusive for the ultra-lean case of ϕ = 0.4 as well as the rich cases beyond ϕ = 1.4, for which a consistent trend is not observed. Recognizing that the lean flammability limit for hydrogen/air mixtures at atmospheric pressure is about ϕ = 0.17, and that increasing pressure could elevate this limit due to enhanced three-body termination reactions, it is reasonable to anticipate the occurrence of local extinction and possibly also re-ignition, which would introduce additional factors in the flame propagation that are not amenable to direct interpretation. Regarding the rich mixtures, we note that while diffusional-thermal cellular instability is suppressed for them, the corresponding pulsating instability is activated and its coupled effects with the hydrodynamic cells have yet to be understood.

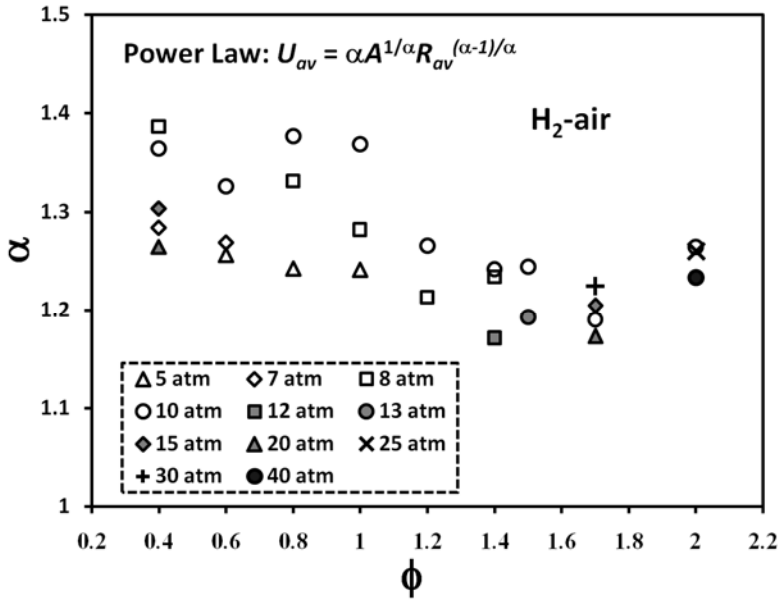

Figure 16: Experimental acceleration exponents for H_2/air at various pressures and equivalence ratios

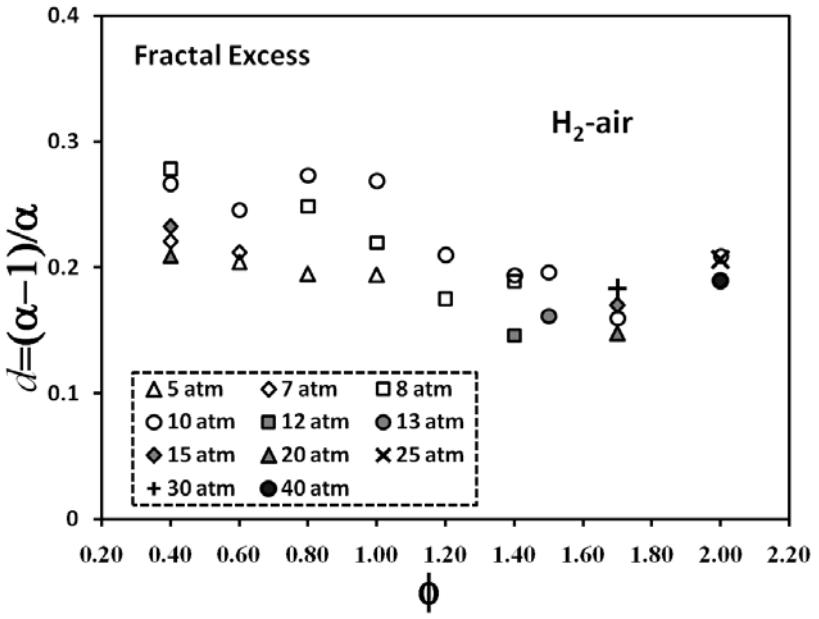

Figure 17: Experimental fractal excess for H_2/air at various pressures and equivalence ratios

Recognizing the potential complication due to diffusional-thermal effects in the interpretation of hydrodynamic instability on the self-similar propagation, it is prudent to consider equidiffusive mixtures for which these effects are suppressed. For hydrogen/air mixtures this is close to the stoichiometric value of ϕ = 1. Figure 16 shows that the acceleration exponent for such mixtures assumes a maximum value of about α = 1.37, occurring at 10 atm pressure. This value, determined in a manner that can be considered to be rigorous based on the current understanding and state-of-the-art investigation, is close to α = 3/2, the value purportedly related to the concept of self-turbulization.

Having determined the acceleration, we plot in Figure 17 the fractal excess, $d = 1 - 1/\alpha$, showing the approach to d = 1/3 for the high-pressure, stoichiometric mixture.

4.3 Effects of Stretch

Although we have experimentally demonstrated the self-similar propagation for wrinkled H_2/air flames, the theoretical formulation is really based on the fact that the laminar flame speed is constant. Since the propagation speeds of unwrinkled lean and rich H_2/air flames ($Le < 1$ and $Le > 1$) respectively increase and decrease with the stretch rate, which however cannot be readily quantified at the local level for the wrinkled flame, this effect on the acceleration exponent determined needs to be assessed. Recognizing that the stretch effect decreases with pressure due to reduced flame thickness, its effect at 1 atm, the lowest pressure in the present study, should serve as the upper limit of its influence. Figure 18 plots the flame velocity versus flame radius for H_2/air flames at 1 atm. Note that at 1 atm, all flames are smooth (stable), therefore their propagation should follow the flame evaluation equation of laminar flame, for which the flame speed varies approximately linearly with the strain rate [27] and as such does not vary in any power-law manner. However, in order to assess the magnitude of such an influence, we have fitted the results locally in the propagation regime of interest. It is seen that the estimated

acceleration exponent varies from 0.93 at $\phi = 0.6$ to 1.07 at $\phi = 1.0$, to 1.14 at $\phi = 2.0$, implying the influence is not large. Since this influence will further substantially decrease with increasing pressure, it is concluded that the stretch effect on the acceleration exponents determined is minor.

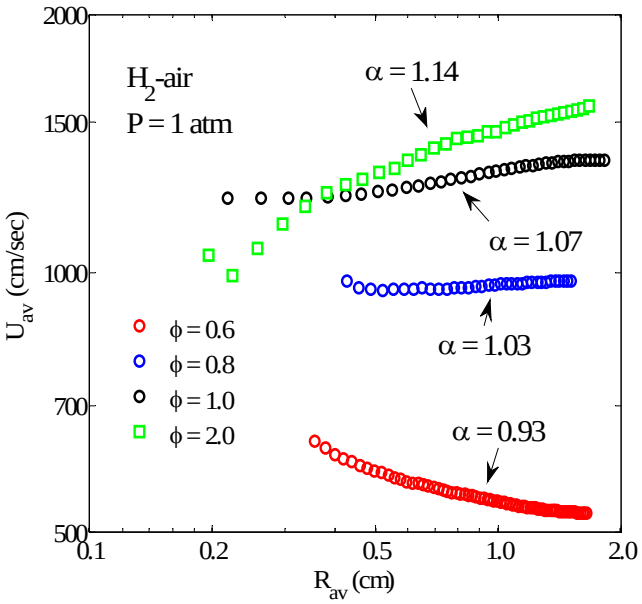

Figure 18: Flame acceleration and deceleration of laminar H_2/air flames at 1 atm due to stretch

5. Concluding Remarks

Two goals were accomplished in the present study. First, we have critically evaluated the extent of rigor in the various claims of self-similarity in previous experimental and computational studies of the self-acceleration of expanding spherical flames, particularly on the attainment of 3/2 for the power-law acceleration exponent. Our conclusion is that the evidences presented in some of these prior studies were not rigorously interpreted. The extent of arbitrariness is particularly discouraging in the exuberant yet unjustified claim of the 3/2 exponent, motivated by the initial suggestion of Gostintsev based on results of uncertain accuracy, and by the attractiveness of its potential implication on self-turbulization. The ripple effect of a weakly substantiated, or even unsubstantiated, claim of a potentially novel scientific concept, periodically reinforced by further studies biased to support the concept, is sobering.

Being mindful of the above concerns, we have designed, conducted and analyzed our experiments with considerable caution and thoroughness. Our results suggest that self-similarity, subsequent to the initial transient, most likely exists. Our power-law exponent, however, still seems to depend on the system pressure and the intensity of the diffusional-thermal instability, and as such has not reached the hydrodynamic, flame-sheet limit. As such, further studies on this scientifically important issue are merited.

Acknowledgments

This research was supported by the microgravity combustion program of NASA.

References

[1] V.V. Bychkov, M.V. Liberman, Physical Review Letters 76 (1996) 2814-2817.
[2] S.I. Blinnikov, P.V. Sasorov, Physical Review E 53 (1996) 4827-4841.
[3] Y.A. Gostintsev, A.G. Istratov, V.E. Fortov, Doklady Akademii Nauk 353 (1997) 55-56.
[4] B.B. Mandelbrot, Journal of Fluid Mechanics 62 (1974) 331-358.
[5] B.B. Mandelbrot, Journal of Fluid Mechanics 72 (1975) 401-416.
[6] K.R. Sreenivasan, R. R., C. Meneveau, Proceedings of the Royal Society A A421 (1989) 79-108.
[7] K.R. Sreenivasan, C. Meneveau, Journal of Fluid Mechanics 173 (1986) 357-386.
[8] K.R. Sreenivasan, Physica D 38 (1989) 322-329.
[9] C.D. Lind, J.C. Whitson, Explosion Hazards Associated with Spills of Large Quantities of Hazardous Materials, Phase II, 1977.
[10] Y.A. Gostintsev, A.G. Istratov, Y.V. Shulenin, Combustion Explosion and Shock Waves 24 (1988) 63-70.
[11] Y.A. Gostintsev, A.G. Istratov, N.I. Kidin, V.E. Fortov, High Temperature 37 (1999) 306-312.
[12] Y.A. Gostintsev, V.E. Fortov, Y.V. Shatskikh, Physical Chemistry 397 (2004) 141-144.
[13] D. Bradley, Combustion and Flame 124 (2001) 551-559.
[14] M.Z. Haq, Journal of Heat Transfer 127 (2005) 1410.
[15] O.C. Kwon, G. Rozenchan, C.K. Law, Proceedings of the Combustion Institute 29 (2002) 1775-1783.
[16] L. Filyand, G. Sivashinsky, M. Frankel, Physica D: Nonlinear Phenomena 72 (1994) 110-118.
[17] W.T. Ashurst, Combustion Theory and Modelling 1 (1997) 405-428.
[18] R. Aldredge, B. Zuo, Combustion and Flame 127 (2001) 2091-2101.
[19] Z. Olami, I. Procaccia, R. Zeitak, Physical Review. E, Statistical Physics, Plasmas, Fluids, and Related Interdisciplinary Topics 52 (1995) 3402-3414.
[20] Z. Olami, B. Galanti, O. Kupervasser, I. Procaccia, Physical Review E 55 (1997) 2649-2663.
[21] B. Galanti, O. Kupervasser, Z. Olami, I. Procaccia, Physical Review Letters 80 (1998) 2477-2480.
[22] M.A. Liberman, M.F. Ivanov, O.E. Peil, D.M. Valiev, L.-E. Eriksson, Physics of Fluids 16 (2004) 2476-2482.
[23] V. Karlin, G. Sivashinsky, Combustion Theory and Modelling 10 (2006) 625-637.
[24] V. Karlin, G. Sivashinsky, Proceedings of the Combustion Institute 31 (2007) 1023-1030.
[25] R. Fursenko, K. Pan, S. Minaev, Physical Review E 78 (2008) 056301.
[26] K.L. Pan, R. Fursenko, Physics of Fluids 20 (2008) 094107.
[27] A.P. Kelley, C.K. Law, Combustion and Flame 156 (2009) 1844-1851.